# Observations of TOPEX/POSEIDON Orbit Errors Due to Gravitational and Tidal Modeling Errors Using the Global Positioning System

**B. J. Haines, E. J. Christensen, J. R. Guinn and R. A. Norman**
**Jet Propulsion Laboratory, California Institute of Technology**
**Pasadena, California 91109 USA**

**J. A. Marshall**
**NASA Goddard Space Flight Center**
**Greenbelt, Maryland 20771 USA**

## INTRODUCTION

Satellite altimetry is faced with the challenge of measuring subtle variations in the dynamic topography of the world's oceans with cm-level accuracy. The TOPEX/Poseidon (T/P) mission was designed to resolve these signals by measuring the radial component of the orbit with an accuracy of 13 cm, or better, in a root-mean-square (RMS) sense, Owing to major advances in precision orbit determination, the actual level of performance is estimated to be nearly an order of magnitude better than that [e.g., *Tapley et al.*, 1994a]. This is primarily clue to improvements in the gravity model for the Earth, including the tide model, and the effectiveness of the 3 precision tracking systems carried on the spacecraft (SCC next section). This paper summarizes the results obtained from a comparison between two distinct types of T/P orbits: classical dynamic orbits and GPS-based reduced-dynamic orbits. Surface manifestations of the relative spatial and temporal behavior of these orbits are described in terms of their effect on altimetric observations of dynamic topography.

## DYNAMIC AND REDUCED-DYNAMIC ORBITS

The orbit height measurements that appear on the T/P mission geophysical data records are computed using data from a global network of international satellite laser ranging (SLR) stations and French radiometric Doppler (DORIS) beacons [e. g., *Tapley et al., 1994a].* Inasmuch as they are computed using a classical dynamical orbit determination technique, their error characteristics are determined in large part by the force models used to integrate the equations of motion. On the other hand, kinematic orbits depend only on the tracking metric to define the trajectory of a satellite and are therefore limited solely by periods of restricted observability and errors associated with the tracking data.

To take advantage of the continuous 3-D data coverage afforded by the GPS Demonstration Receiver (GPS-DR) on board '1'/1', the strengths of the dynamic and kinematic methodologies have been combined in what is referred to as the reduced-dynamic technique, wherein small, local geometric corrections are made to a previously computed

dynamic orbit [*Bertiger et al.,* 1994]. Insofar as reduced-dynamic GPS orbits have a kinematic component, comparisons between GPS and SLR-DORIS dynamic orbits can reveal deficiencies in the dynamic models and errors associated with the tracking systems.

## METHODOLOGY

For the current analysis, a time series of radial orbit differences between the NASA Precise Orbit Ephemerides (POE) [*Tapley et al.*, 1994a] and GPS reduced-dynamic orbits for the time span from February 28, 1993 to January 30, 1994 was examined. This time period covers the T/P 10-day repeat cycles 17 through 50 and was chosen because it represents a nearly contiguous span of high quality GPS-DR data. (The GPS-DR tracked in precise dual-frequency mode 86% of the time.) We then averaged the data over - 10-day moving windows centered at 3.3 day intervals (the length of a T/P sub-cycle). This resulted in 99 frames of global radial orbit differences spanning a period of almost one year.

The data in each frame were interpolated onto a uniform global geographic grid (5° *X* 5°) by employing a least-squares collocation technique [e.g., *Moritz*, 1980] using a Gaussian signal covariance function with a maximum value of 4 $cm^2$, a decorrelation distance of 6°, and a white-noise covariance of 4 $cm^2$. Empirical orthogonal functions (EOFs) [e.g., *Priesendorfer*, 1988] were then computed to provide insight into the dominant modes of variability.

## RESULTS AND CONCLUSIONS

Depicted in Figures 1 and 2 are geographic distributions of the mean and standard deviation of the radial orbit differences based on the 99 gridded maps. Maps corresponding to both the original NASA POE (based on the JGM-2 gravity model [*Nerem et al., 1994]*) and the new POE (based on JGM-3 [*Tapley et al.*, 1994b] and improved tide models) are shown. Prominent in Figure 1 (a) is a large meridional feature which is due primarily to errors in the JGM-2 gravity model [e.g., *Christensen et al.*, 1994]. This is corroborated by Figure 1 (b) which shows that the meridional feature is significantly attenuated when the new JGM-3 POEs are used. Note that the map still has a dominant north-south hemispherical feature which is a manifestation of a slight shift along the Earth spin axis [see also *Marshall et al.*, 1995]. The source of this "Z-shift" is still under investigation.

Superimposed on these stationary features are temporally varying geographically correlated orbit errors (Figure 2). Using EOF analysis to segregate the variability into orthogonal components, we determined that the dominant modes of variability correspond to periodic shifting in the center-of-figure. Shown in Figure 3, for example, are geographic representations of the first 6 modes of variability for the differences of the JGM-2 POE and GPS-based orbits. The first mode--explaining 25 % of the overall variance--is comprised primarily of a long-term variation in the "Z-shift". This is corroborated in Figure 4, which shows a comparison of the Mode 1 amplitude time series and the cycle-by-cycle averages of the body-fixed Z-coordinate differences (JGM-2 POE vs. GPS - based orbit). The second and third modes correspond to shifts along orthogonal axes in the equatorial plane and explain 18 and 11 % of the overall variance respectively.

Modes 5–6 are much less energetic, each explaining 3–6 % of the overall variance. Examination of the spectra for these modes reveals a dominant peak at the -60 day period (Figure 5). Using Fourier analysis, *Marshall et al. [1995]* have shown that the temporal errors at this frequency are attributable to aliased errors in the non-resonant (i .e.,

background) components of the principal lunar (M2) and solar (S2) tides which arc applied in the POE computations [see also *Bettadpur and Eanes*, 1994].

We repeated the EOF anal ysis, replacing the JGM-2 POE with the JGM-3 POE. Large-scale hemispherical variations still characterize the first 3 modes. The first two modes share most of the energy—27% and 23% respectively—but neither correspond closely to the Z-shift. Like the JGM-2 comparison, 60-day variations are present in higher modes, though the overall energy at the M2/S2 alias frequency is reduced owing to the application of an improved background tide model [see also *Marshall et al., 1995]*. A preliminary comparison of the JGM-3 POE with a new set of improved GPS-based orbit shows even less variability, indicating that the solutions based on entirely different data types and orbit determinant ion techniques arc converging as the force and measurement models improve.

Also noteworthy arc the EOF results which suggest that the most energetic spatio-temporal variabilities associated with the orbit errors are not tide related, rather they have their origin in the definition of the ostensible geocenter. The Z-shift variations are very important, because they can introduce basin-to-basin errors in the ocean topography that direct] y impact est imates of seasonal steric changes. We note that, at this writing, we have no evidence to suggest that the geocenter problems arc duc to dynamic model errors associated with the POE; in fact, they likely arise from measurement model errors attributable to either or both of the orbit solutions contributing to the difference. These issues arc currently under investigation [e.g., *Guinn et al.*, these proceed ings].

***Acknowledgment.*** The research described in this paper was carried out in part at the Jet Propulsion Laboratory, California Institute of Technology, under contract with the National Aeronautics and Space Administration. We are grateful to Ernst Schrama at the Delft University of Technology for providing the least-squtires collocation software.

## REFERENCES

Bertiger, W. 1.. *et al.*, G P S, precise tracking of '1 'OPEX/Poseidon: Results and implicat ions, *J. Geophys. Res.* 99(C 12), 24,419-24,464, 1994.

Bettadpur, S. V., and R. J. Eanes, Geographical representation of radial orbit perturbations duc to ocean tides: Implications for satellite orbit determination, *J. Geophys. Res. 99*(C1 2), 24,883-24,894, 1994.

Christensen, E. J., B. J. Haines, K. C. McColl and R. S. Nerem, Observations of geographical] y correlated orbit errors for TOPEX/Poseidon using the global positioning system, *Geophys. Res. Ltr.* ***21(9), 2 175–2 178,*** 1994.

Guinn, J., *et al.*, TOPEX/Poseidon precision orbit determination using combined GPS, SLR and DORIS, these proceedings, 1995.

Marshal], J. A., *et* al., The temporal and spatial characteristics of TOPEX/Poseidon radial orbit error, *J. Geophys. Res.*, in press, 1995.

Nerem, R. S., *et al.*, Gravity model development for '1'OPF.X/Poseidon: Joint gravity models 1 and 2, *J. Geophys. Res.* ***99(C 12), 24,421 –24,447,*** 1994.

Moritz, H., *Advanced Physical Geodesy,* Herbert Wichman Verlag, Karlsruhe, Germany, 1980,

Priesendorfer, R. W., *Principal component analysis in meteorology and oceanography,* Elsevier Science Publishers, 1988.

Tapley, B. D., *et al.*, Precision orbit determination for TOPEX/Poseidon, *J. Geophys. Res.* ***99(C 12), 24,383-24,404, 1994a.***

Tapley, B. D., M. M. Watkins, et al., The JGM-3 gravity model, *Annales Geophysicae, 12, Suppl. 1, C192, 1994b.*

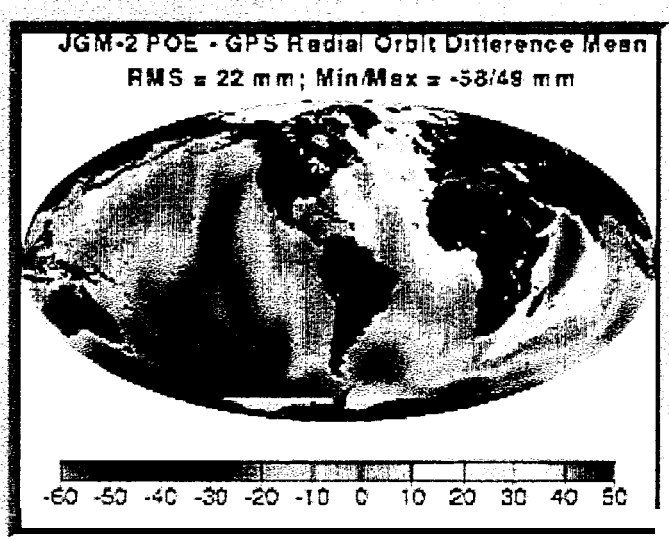


Figure 1(a)

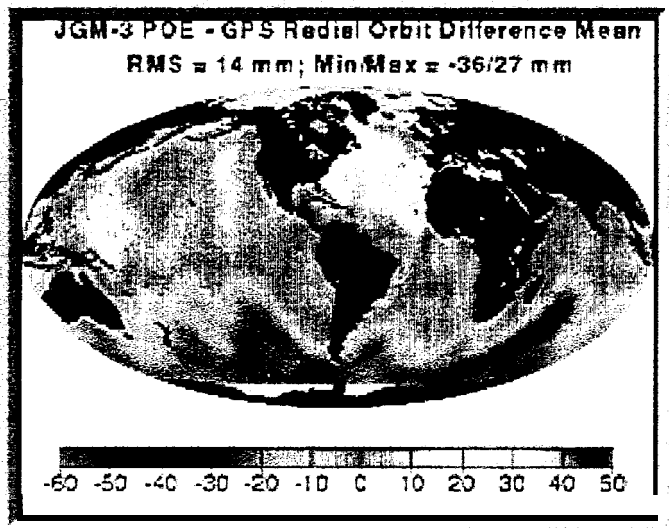


Figure 1(b)

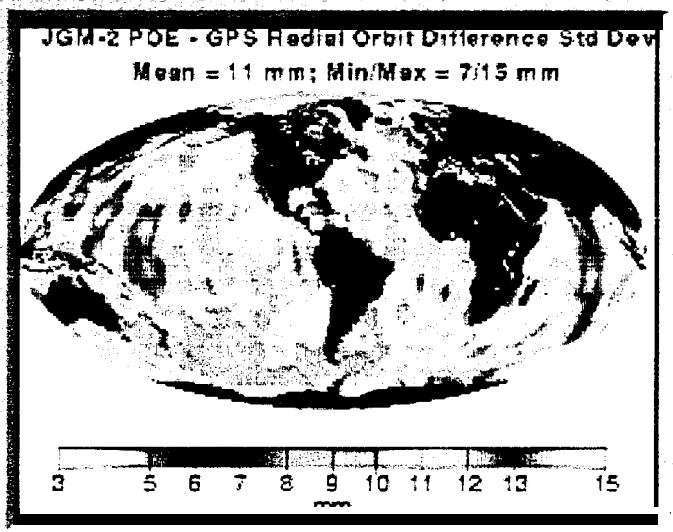


Figure 2(a)

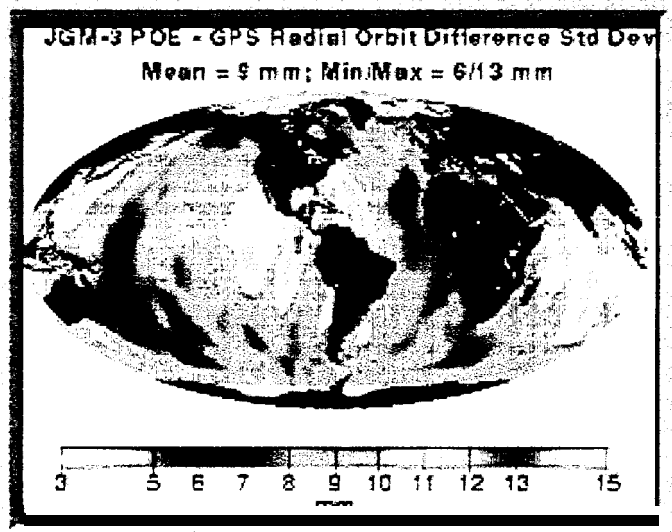


Figure 2(b)

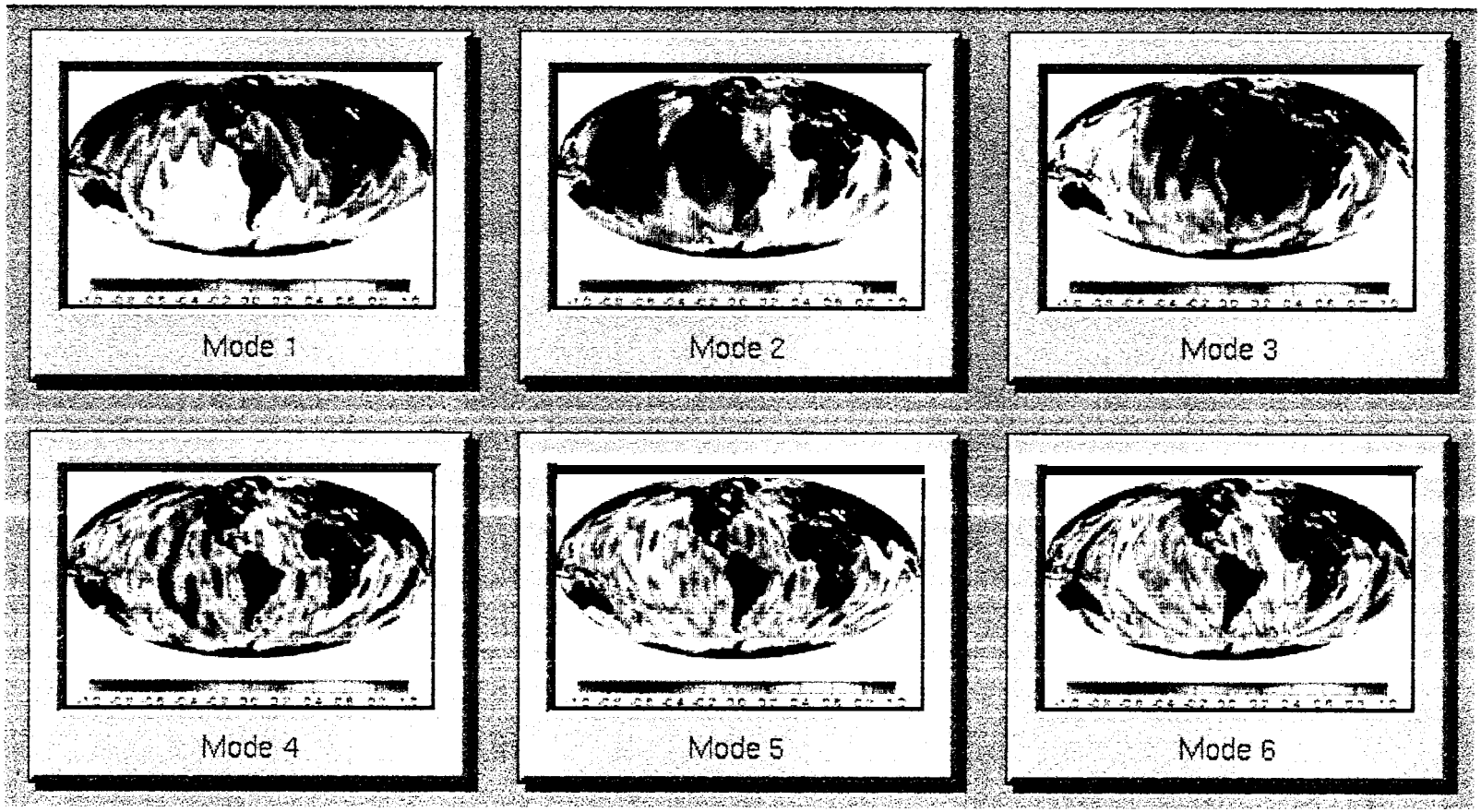


Fig. 3. Spatial representations (eigenvectors) of the 6 largest modes of variability for the JGM-2 POE vs GPS reduced dynamic orbit comparison from empirical orthogonal function analysis. The maps have been normalized so that the largest excursion is +/- 1. Note that the first 3 modes are characterized by large-scale features indicative of shifting in the center of figure (i.e., geocenter). Modes 4 through 6 contain shorter-wavelength features, some of which are attributable to errors in the JGM-2 POE background models of the principal lunar and solar tides. (This is further evidenced in Fig. 5 )

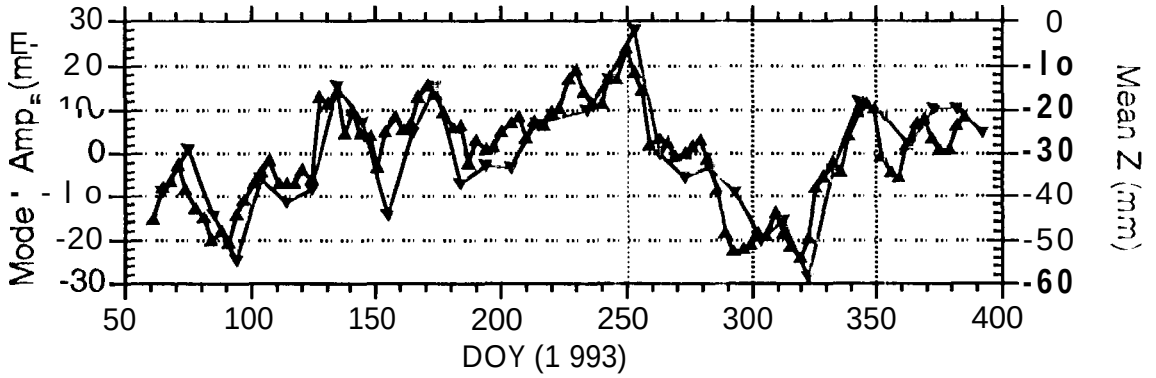


**Fig.** 4. The blue line shows the amplitude time series of the primary EOF mode for the JGM-2 POE - GPS reduced dynamic orbit differences. The red line shows the cycle-averaged body-fixed Z-offset for the same two orbit solutions. The high correlation corroborates that long-term changes in the Z-shift (compare also Figure 3a) comprise the primary mode of spatio-temporal variability.

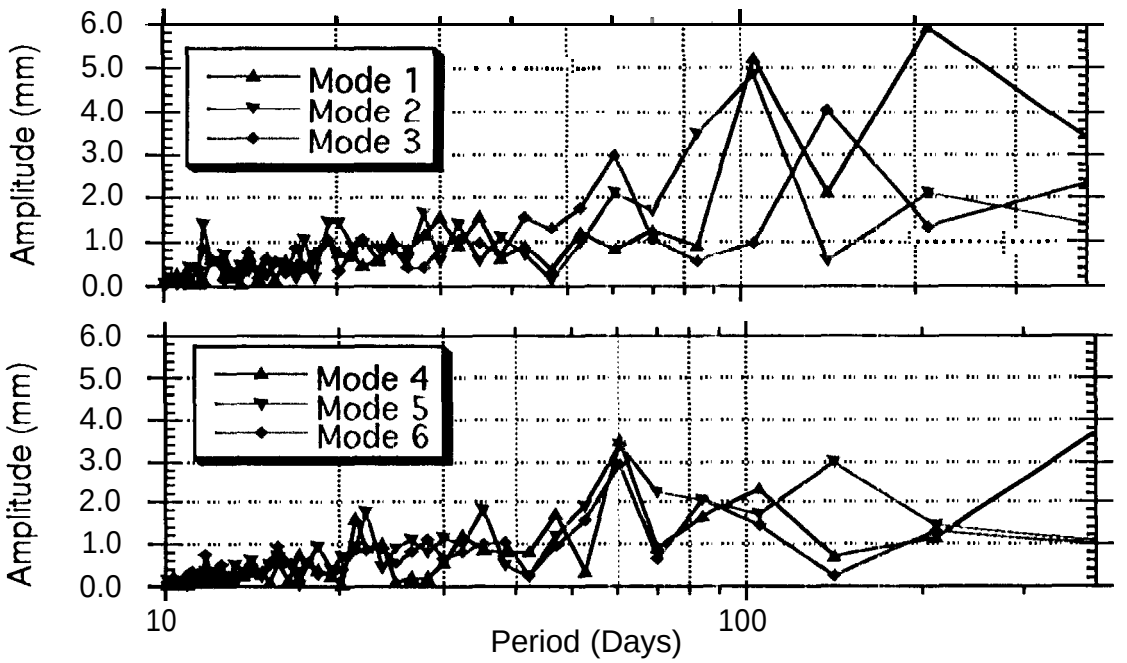


Fig. 5. Spectra of the amplitude time series for the EOF modes 1--3 (top panel) and 4--6 (bottom panel) for the JGM-2 POE - GPS reduced dynamic orbit differences. The first three modes, corresponding to center-of-figure motion, are characterized by long-term variations (> 100 d) while modes 4-6 exhibit 60-day variability associated with the M2/S2 tidal alias.